Effect of human-driven, autonomous, and connected autonomous vehicles on geometric highway design

Zawar Hussain Khan, Faryal Ali, Ahmed B. Altamimi, & Thomas Aaron Gulliver

2025

Original citation:
Khan, Z. H., Ali, F., Altamimi, A. B., & Gulliver, T. A. (2025). Effect of human-driven, autonomous, and connected autonomous vehicles on geometric highway design. *Alexandria Engineering Journal*, *127*, 1073–1080.
https://doi.org/10.1016/j.aej.2025.07.013

Alexandria Engineering Journal 127 (2025) 1073–1080

Contents lists available at ScienceDirect

Alexandria Engineering Journal

journal homepage: www.elsevier.com/locate/aej

Original article

Effect of human-driven, autonomous, and connected autonomous vehicles on geometric highway design

Zawar Hussain Khan [a], Faryal Ali [b,*], Ahmed B. Altamimi [a], Thomas Aaron Gulliver [b]

[a] College of Computer Science and Engineering, University of Ha'il, Ha'il, Saudi Arabia
[b] Department of Electrical and Computer Engineering, University of Victoria, Victoria, BC V8W 2Y2, Canada

ARTICLE INFO

Keywords:
Spring-mass system
Horizontal curves
Geometric design
Microscopic traffic model
Human-driven Vehicles (HVs)
Autonomous Vehicles (AVs)
Connected Autonomous Vehicles (CAVs)

ABSTRACT

Highway geometric design plays a crucial role in maintaining traffic safety and operational efficiency. The number of Autonomous Vehicles (AVs) and Connected Autonomous Vehicles (CAVs) on highway networks has increased in recent years. In this study, a traffic model is developed from a spring-mass system theory perspective to investigate traffic dynamics on horizontal highway curves. The Intelligent Driver (ID) model is based on a constant exponent δ to characterize driver response, which is unrealistic. By utilizing a spring-mass system analogy, the proposed model provides a more accurate and realistic representation of traffic. This model is used to evaluate the behavior of Human-driven Vehicles (HVs), AVs, and CAVs over a 1300 m circular road. The results obtained show that CAVs have better performance compared to HVs and AVs on horizontal curves, leading to better understanding of safety and efficiency on roads. Further, CAVs improve energy efficiency and emission reduction, contributing to effective and sustainable transportation systems. In addition, the results indicate that the proposed model has better performance compared to the ID model.

1. Introduction

The rapid urbanization worldwide and the increasing number of vehicles have exacerbated traffic problems such as congestion, pollution, management, and safety. Traditional traffic control and management technologies have had limited effect in mitigating these issues [1]. According to the US Department of Transportation, in 2015, 94% of traffic accidents in the United States were due to human error [2]. Further, about 80% of traffic accident deaths are due to the lack of connectivity between vehicles [3]. It has been shown that driving systems can reduce or eliminate human error associated with vehicle collisions [4]. Autonomous Vehicles (AVs) and Connected Autonomous Vehicles (CAVs) have recently been introduced on highway networks. These vehicles are equipped with driver assistance systems ranging from basic cruise control to communication with other vehicles (V2V) or other systems (V2X) without human intervention [2,5]

AVs navigate autonomously using sensors and communications without human involvement. They perform driving tasks based on sensor data and internal systems [3]. AVs respond in real time to received data and use intelligent software to ensure passenger safety, comfort, and operational efficiency [6]. Automated driving systems encompass both hardware, such as sensors, and software, such as trajectory planning systems. They assist drivers in dynamic driving tasks including monitoring the driving environment and controlling lateral and longitudinal motion [7]. CAVs are a promising technology to reduce traffic accidents and emissions, and improve traffic efficiency [8]. They navigate using sensors to observe the surrounding environment, control systems to make decisions, and actuators for operations such as steering and braking [3]. Advanced sensors such as Lidar, millimeter-wave radar, and cameras allow CAVs to perceive their surroundings and identify objects such as pedestrians and traffic signals in real time [9]. Wireless communications technology such as 5 G and Wi-Fi provide connectivity with nearby vehicles to improve safety and road capacity by adjusting the distance headway between vehicles [8,10]. According to the Virginia Department of Transportation, highway capacity increases by approximately 28% and 92% with AVs and CAVs, respectively, compared to Human-driven Vehicles (HVs) [3].

Highway geometric design plays a critical role in traffic safety and operational efficiency. In [11], the influence of highway geometric design on vehicle performance was shown to be significant. The impact of AVs on road design was explored in [12]. It was suggested that AVs require fewer geometric design specifications which lead to lower costs

* Corresponding author.
E-mail addresses: z.hussain@uoh.edu.sa (Z.H. Khan), faryalali@uvic.ca (F. Ali), altamimi.a@uoh.edu.sa (A.B. Altamimi), agullive@uvic.ca (T.A. Gulliver).

https://doi.org/10.1016/j.aej.2025.07.013
Received 29 April 2024; Received in revised form 14 August 2024; Accepted 8 July 2025
Available online 17 July 2025

Fig. 1. Spring-mass phenomenom in traffic flow.

and higher traffic speeds than with HVs. However, AVs and CAVs have poorer performance on horizontal or vertical curves [3]. Horizontal curves are used on highways for alignment or changes in direction while vertical curves are used to change the slope [13]. Moreover, the adhesion between the tires and the road surface affects acceleration and deceleration. It was shown in [14] that AVs can degrade traffic safety when the lane width is reduced. Narrow lanes reduce the superelevation runoff which compromises skid resistance, and AVs may fail to capture road surface conditions on inclines [3]. The banking of horizontal curves so vehicles can safely traverse them is known as superelevation, and the superelevation runoff is the length of roadway required to transition the outside-lane cross slope from zero to full superelevation and vice versa [15].

The effect of AVs on vertical curves was investigated in [2] by considering the difference in reaction time between AVs and HVs. The effect of AVs on geometric elements such as sight distance and length of vertical curves was examined in [16] based on the reaction time and acceleration. However, there has been very little investigation of the impact of AVs and CAVs on geometric design, particularly horizontal highway curves. The main purpose of horizontal curves is to provide smooth transitions between straight road sections [13]. Thus, a traffic model is developed to investigate traffic flow on horizontal curves and determine the behavior of AVs and CAVs.

Three types of models are used to describe traffic flow behavior: microscopic, macroscopic, and mesoscopic. Microscopic models are employed to describe the behavior of individual vehicles. They consider the speed, position, and headway of a vehicle, and their dynamics are typically characterized using ordinary differential equations that are easy to solve [17,18]. Macroscopic models consider average traffic density and speed and employ partial differential equations [19]. Mesoscopic models are a hybrid of microscopic and macroscopic models [20].

Various traffic models have been developed since the first microscopic car following models [21,22]. A traffic model based on the safe distance headway was developed in [23]. According to this model, drivers maintain a safe distance according to forward conditions to avoid collisions [24]. In [25], a model based on the relationship between speed and distance headway was introduced. With this model, a larger distance headway results in higher speeds and the distance headway is small during congestion [26]. However, it produces uniform acceleration for changes in traffic conditions which is inaccurate and unrealistic. In [27], a model based on driver reaction was proposed to reduce traffic congestion and improve stability. The model in [28] considers the speed difference in various traffic conditions. However, these models can cause collisions as they can produce high speeds when the distance headway is smaller than the safe distance headway.

A model incorporating psychological-physical driver response to large changes in traffic conditions was developed in [29]. However, this model is very complex because it has a large number of parameters [30]. In [31], a model with a smaller number of parameters was presented. Unfortunately, it produces constant acceleration and deceleration which is unrealistic [32]. The Intelligent Driver (ID) model was developed in [33] to provide realistic acceleration and deceleration. This model characterizes traffic behavior based on driver response considering speed and distance headway. It is widely used to analyze the stability of automated and connected vehicles. An improved ID model was presented in [34]. It employs following and leading vehicle information to describe traffic behavior in a connected environment. However, it cannot characterize CAVs in actual traffic conditions [35]. A model to guide connected vehicles through traffic signals was proposed in [36].

Several macroscopic models have been developed to characterize traffic behavior. Lighthill, Whitham, and Richards [37,38] developed a model for traffic behavior at equilibrium. However, it ignores traffic flow in non-equilibrium conditions and adjusts vehicle speed in zero time [39]. The Payne–Whitham model [40,41] considers spatial-temporal stop and go traffic behavior. The model in [42] focuses on anisotropic traffic characteristics. Lattice hydrodynamic models were developed in [43,44] to characterize traffic density.

The models discussed above are based on fluid dynamics theory. Thus, they treat traffic flow as a compressible fluid based on the principles of fluid dynamics [45,46]. However, vehicle acceleration and deceleration behave like a mechanical system, i.e. a spring-mass system. For example, vehicles accelerate when the distance headway is larger than the safe distance headway and decelerate when it is smaller than the safe distance headway. Thus, a traffic model based on mechanical systems is proposed here. It is used to evaluate traffic behavior on a horizontal curve, in particular, the behavior of HVs, AVs, and CAVs.

The remainder of this paper is organized as follows. The spring-mass system model is presented in Section 2. The behavior of HVs, AVs, and CAVs is evaluated in Section 3, and a summary of the paper is given in Section 4.

2. Proposed model

According to the ID model, traffic behavior is a function of speed v, distance headway h, and the difference in speed between following and leading vehicles $\mathscr{D}_v$ [33]

$$\dot{v} = a^*\left(1 - \left(\frac{v}{v^*}\right)^{\delta} - \left(\frac{h^*}{h}\right)^{2}\right), \tag{1}$$

where a^* and v^* are the maximum acceleration and speed, respectively, and h^* is the desired distance headway which can be expressed as

$$h^* = j + v\tau + \frac{v\mathscr{D}_v}{2\sqrt{a^* b^*}} \tag{2}$$

where τ is the time headway, j is the spacing during traffic jams, b^* is the deceleration and δ is the acceleration exponent. In the ID model, driver response to changes in traffic conditions is characterized by δ, which is a constant. Thus, driver behavior is the same for different traffic conditions including horizontal highway curves, whereas the driving environment can significantly influence vehicle movement. This results in unsuitable traffic behavior which is not related to traffic physics.

Driver response is affected by the distance required for vehicles to align to changes in traffic conditions. This is analogous to a spring-mass system. When a force is applied to a mass m attached to a spring, the spring stretches. This stores potential energy in the spring which is released as kinetic energy when the force is removed, causing the mass to oscillate. This is analogous to traffic flow as shown in Fig. 1. When the distance headway h is large, traffic accelerates so the speed increases. When the speed decreases, the distance headway is reduced until the safe distance headway h_s is achieved. Thus, h fluctuates around h_s according to the speed. When h is larger than h_s, vehicles accelerate, and they decelerate when h is smaller than h_s. Considering this analogy between a spring-mass system and traffic behavior, Hooke's law [47] for traffic flow can be expressed as

$$a = \frac{k}{m}(h - h_s) \tag{3}$$

where a is driver response, m is the vehicle mass, and k is the spring constant. The sensitivity defined as $\xi = \frac{k}{m}$ is analogous to the reaction of a driver to changes in traffic conditions.

Fig. 2. Centrifugal force and highway superelevation.

Table 1
Simulation Parameters.

Parameter	Value
Maximum speed, v^*	30 m/s
Time headway, τ	0.5, 1, 2, and 2.5 s
Maximum acceleration, a^*	0.73 m/s^2
Friction coefficient	0.7
Superelevation rate, e	0.036 m
Spacing during jam, j	5 m
Deceleration, b^*	1.67 m/s^2
Vehicle length, l	4.5 m
Reaction time of HVs, ξ	1.6 s
Reaction time of AVs, ξ	0.5 s
Reaction time of CAVs, ξ	0.1 s
Maximum normalized density, $\sigma = \frac{1}{j}$	0.2
Acceleration exponent, δ	1, 4, and 80
Time step, Δt	0.5 s

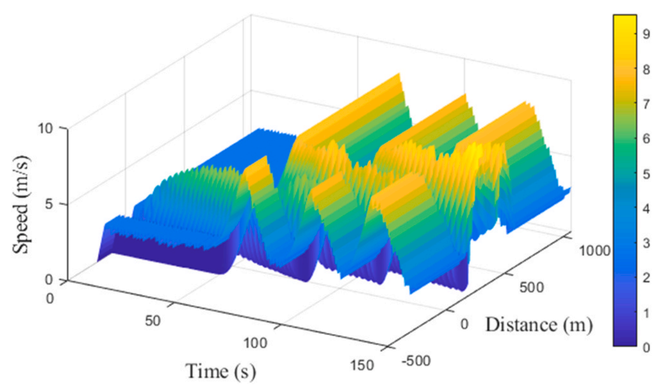

Fig. 3. Temporal and spatial speed with HVs ($\xi = 1.6$ s) at time headway $\tau = 1$ s over a 1300 m circular road.

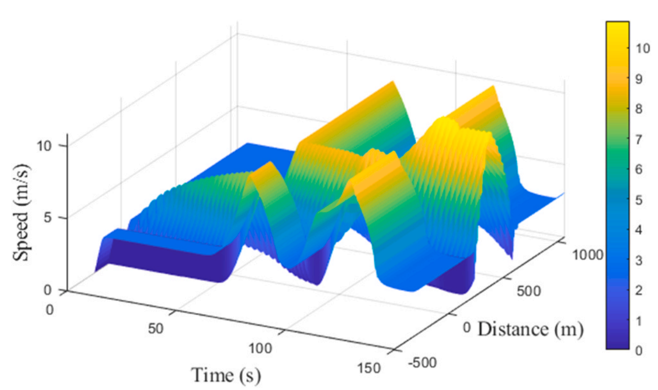

Fig. 4. Temporal and spatial speed with AVs ($\xi = 0.5$ s) at time headway $\tau = 1$ s over a 1300 m circular road.

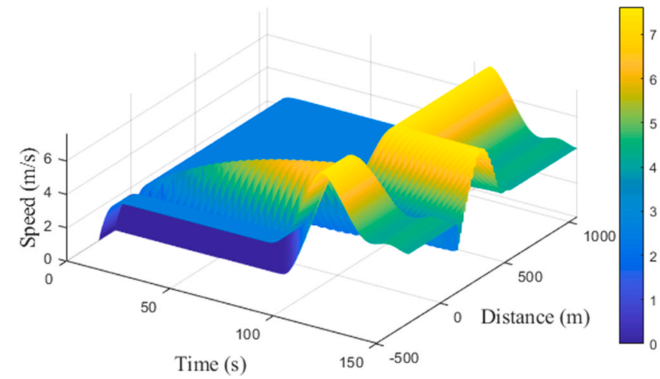

Fig. 5. Temporal and spatial speed with CAVs ($\xi = 0.1$ s) at time headway $\tau = 1$ s over a 1300 m circular road.

It has been shown that AVs react to changes in traffic conditions much faster than HVs [5]. For example, HV reaction time is in the range 1.1 −1.6 s whereas AV reaction time is about 0.5 s and CAVs reaction time is only 0.1 s [5]. From (3), driver response has the form

$$\xi(h - h_s) \tag{4}$$

A large distance headway results in a small traffic density σ, whereas the density is maximum when the distance headway is smallest, i.e. $h = 1/\sigma$ [48]. Traffic flow q is the product of speed and density [1], so (4) can be expressed as

$$\xi\left(\frac{v}{q} - h_s\right) \tag{5}$$

In addition, traffic flow is large with a small time headway τ. Thus, flow is inversely proportional to time headway [19,49], so (5) becomes

$$\xi(v\tau - h_s) \tag{6}$$

The change in distance with time results in a velocity change, which gives $s/\tau = v$ [48]. Thus, (6) can be written as

$$\xi(s - h_s) \tag{7}$$

and from the equation of motion [50]

$$s = v\tau + \frac{1}{2}a\tau^2 \tag{8}$$

Substituting (8) in (7) gives

$$\xi\left(v\tau + \frac{a\tau^2}{2} - h_s\right) \tag{9}$$

A vehicle travelling around a horizontal curve develops a centrifugal force [51]

$$F = \frac{mv^2}{R} \tag{10}$$

where R is the radius of the curve which is given by [52,53]

$$R = \frac{v^2}{g(f + e)} \tag{11}$$

In (11), $g = 9.8$ m/s^2 is the acceleration due to gravity, f is the friction coefficient, and e is the superelevation as shown in Fig. 2. According to the US Federal Highway Administration, e ranges from 0.012 m to 0.036 m and is based on parameters such as climate and traffic speed. The value of e for normal weather conditions and high speeds is larger than for adverse weather conditions and low speeds [54]. Substituting (11) in (10) gives

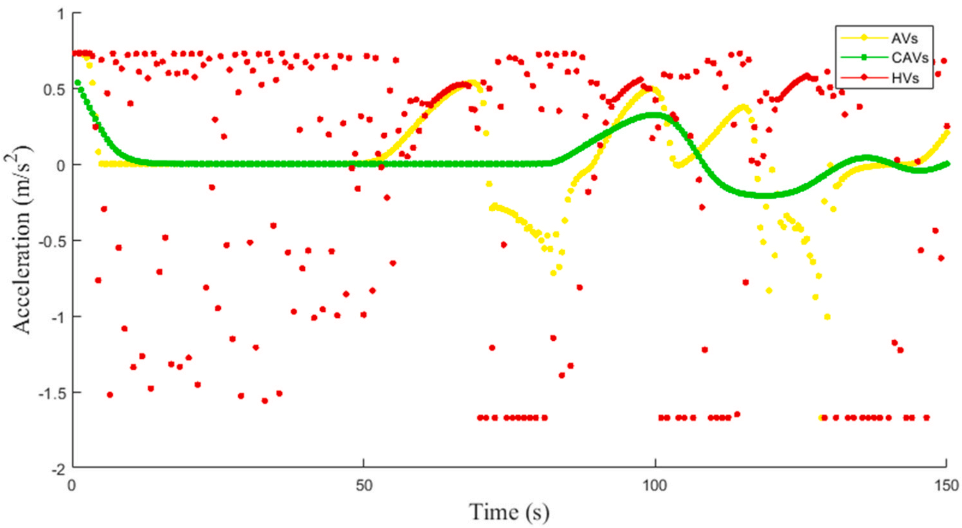

Fig. 6. Temporal acceleration with HVs ($\xi = 1.6$ s), AVs ($\xi = 0.5$ s), and CAVs ($\xi = 0.1$ s) for time headway $\tau = 1$ s over a 1300 m circular road.

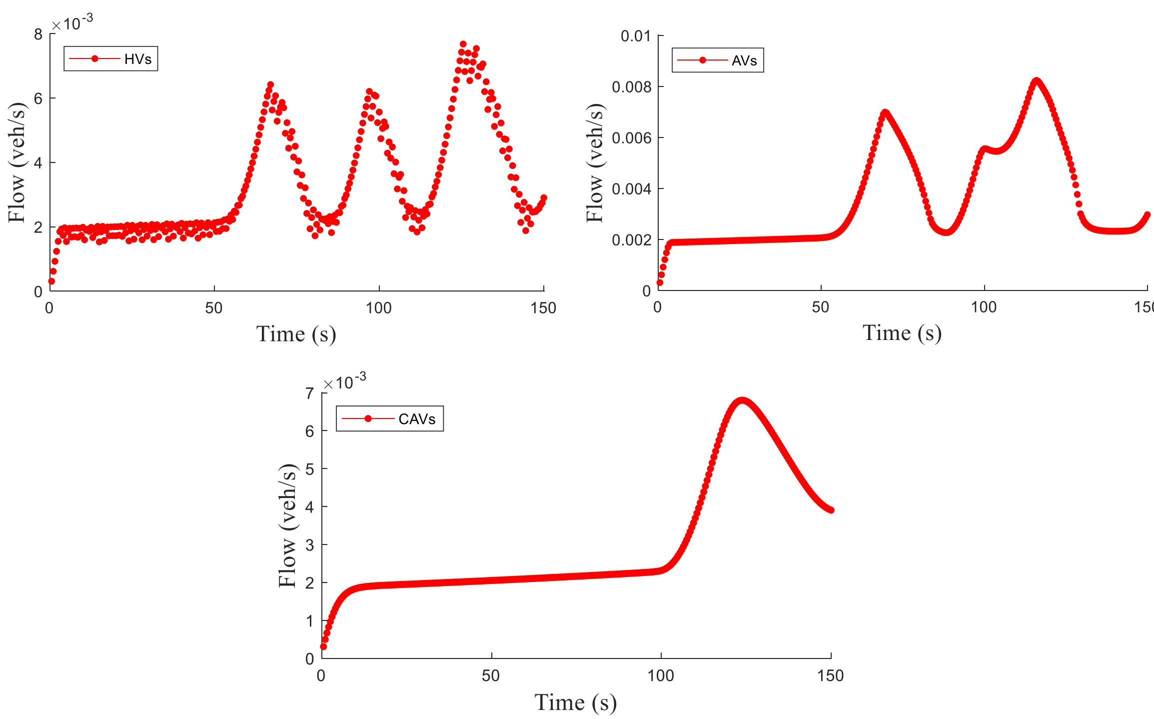

Fig. 7. Temporal flow with HVs ($\xi = 1.6$ s), AVs ($\xi = 0.5$ s), and CAVs ($\xi = 0.1$ s) for time headway $\tau = 1$ s over a 1300 m circular road.

$$a = g(f + e) \tag{12}$$

and using this in (9), we have

$$\xi\left(v\tau + \frac{\tau^2 g(f+e)}{2} - h_s\right) \tag{13}$$

The proposed model is obtained by replacing δ in (1) with (13) which gives

$$\dot{v} = a^*\left(1 - \left(\frac{v}{v^*}\right)^{\xi\left(v\tau + \frac{\tau^2 g(f+e)}{2} - h_s\right)} - \left(\frac{d^*}{d}\right)^2\right). \tag{14}$$

With this model, traffic is characterized based on the reaction time and geometric design which is more realistic than the fixed δ in the ID model. Further, traffic behavior varies according to the geometric design whereas the ID model does not consider the type of road. The traffic flow with the proposed model can be expressed as [26]

$$q = \frac{v}{d_e} \tag{15}$$

where d_e is the distance headway at equilibrium given by

$$d_e = (j + v\tau)\left(1 - \left(\frac{v}{v^*}\right)^{\xi\left(v\tau + \frac{\tau^2 g(f+e)}{2} - h_s\right)}\right)^{-\frac{1}{2}} \tag{16}$$

Substituting this in (15) gives the flow for the proposed model as

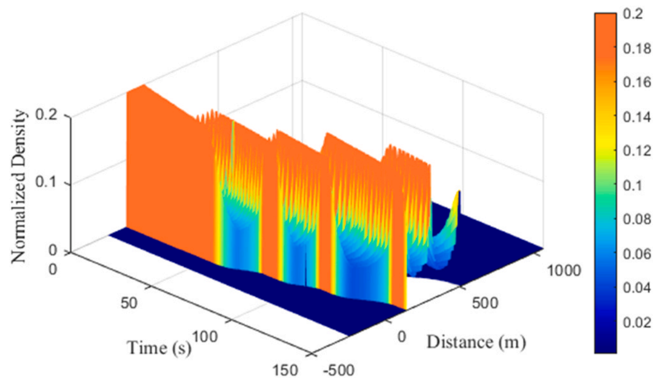

Fig. 8. Temporal and spatial density with HVs ($\xi = 1.6$ s) and time headway $\tau = 1$ s over a 1300 m circular road.

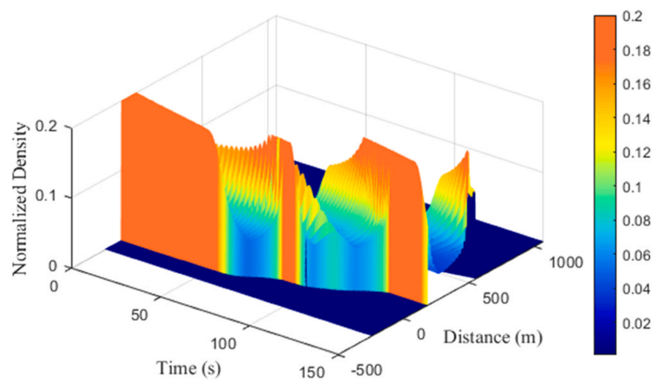

Fig. 9. Temporal and spatial density with AVs ($\xi = 0.5$ s) and time headway $\tau = 1$ s over a 1300 m circular road.

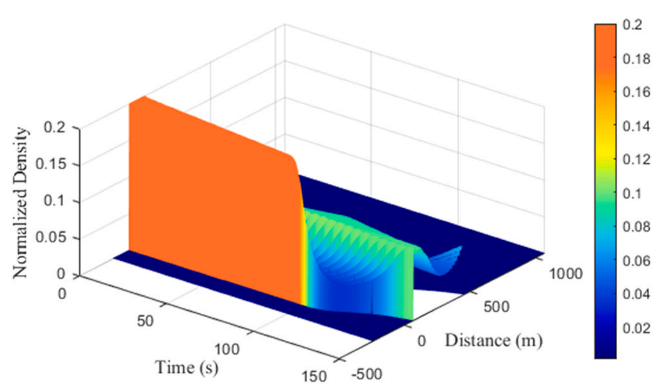

Fig. 10. Temporal and spatial density with CAVs ($\xi = 0.1$ s) and time headway $\tau = 1$ s over a 1300 m circular road.

$$q = \frac{v}{(j+v\tau)\left(1-\left(\frac{v}{v^*}\right)^{\xi\left(v\tau+\frac{\tau^2 g(f+e)}{2}-h_s\right)}\right)^{-\frac{1}{2}}} \qquad (17)$$

Thus, traffic flow is influenced by the geometric design and reaction time. Vehicles with a large reaction time will behave differently on horizontal curves compared to those with a short reaction time. This is more realistic than the ID model which characterizes traffic flow based on a constant δ and so cannot produce acceptable traffic behavior on horizontal curves.

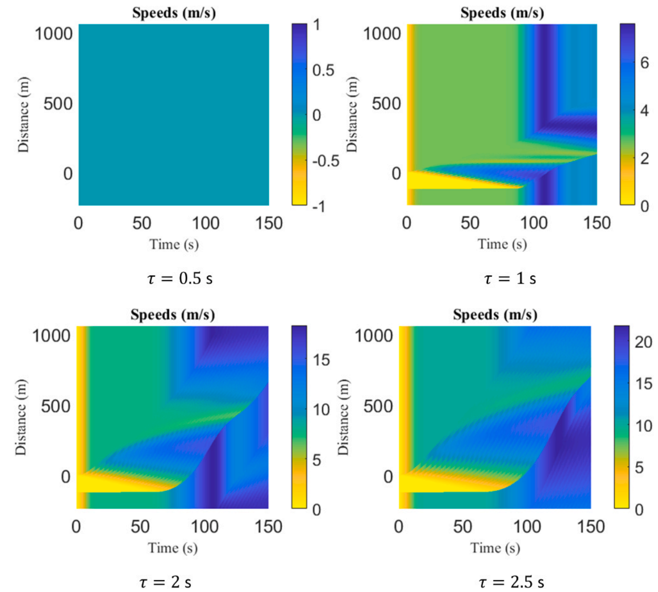

Fig. 11. CAV speed with the proposed model over time and space for $\tau = 0.5$, 1, 2, and 2.5 s.

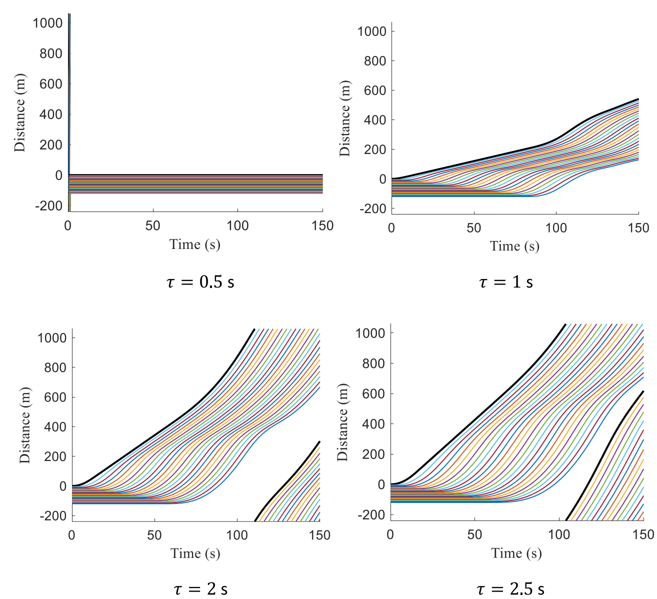

Fig. 12. CAV trajectories over time and space with the proposed model for $\tau = 0.5$, 1, 2, and 2.5 s. The black line shows the trajectory of the 1st vehicle, and the colored lines show the trajectories of the 24 following vehicles.

3. Performance evaluation

In this section, the performance of the proposed model with HVs, AVs, and CAVs is evaluated. In addition, the performance of CAVs is considered with different time headway τ values and compared with the ID model for $\delta = 1$, 4, and 80, as it is typically in the range 1 to ∞ [33]. Results are obtained for a 1300 m circular road and time duration 150 s using the explicit Euler scheme with time step 0.5 s [48]. The friction coefficient employed is 0.7 which is a typical value for dry roads [55,56] and the maximum speed is 30 m/s [48]. The maximum acceleration and deceleration are 0.73 m/s^2 and 1.67 m/s^2, respectively [33]. The time headway is based on the traffic conditions and is typically between 0.5 s and 2.6 s [57]. The vehicle length is 4.5 m [58] and the maximum normalized density is $\frac{1}{j} = 0.2$. Spacing during traffic jams varies

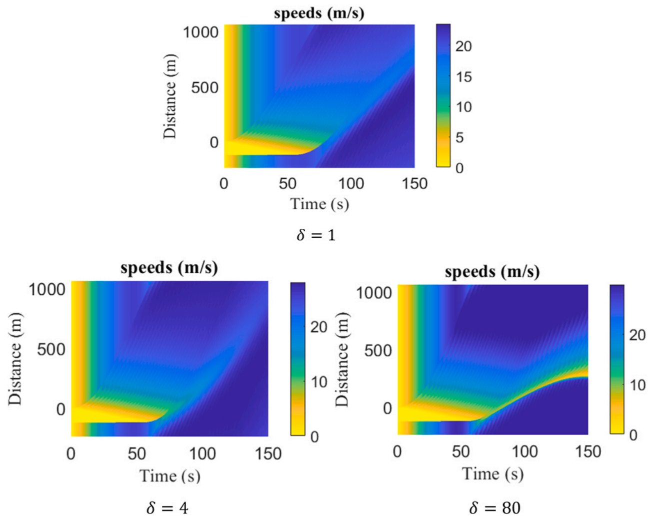

Fig. 13. ID model speed over time and space for $\delta = 1, 4$, and 80.

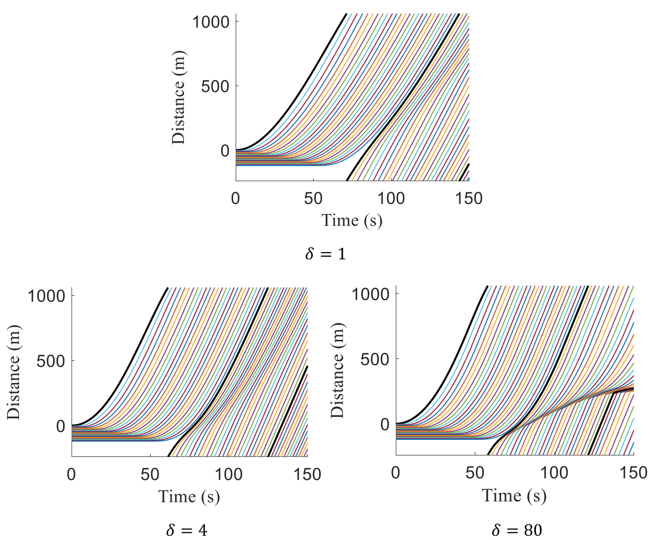

Fig. 14. Vehicle trajectories over time and space with ID model for $\delta = 1, 4$ and 80. The black line shows the trajectory of the 1st vehicle, and the colored lines show the trajectories of the 24 following vehicles.

between 2 m and 7 m [33,48], so 5 m is used here. The simulation parameters are given in Table 1.

3.1. Performance with HVs, AVs, and CAVs

In this section, the performance is evaluated using the proposed model. The speed over a 1300 m circular road for 150 s with HVs, AVs, and CAVs is given in Figs. 3, 4, and 5, respectively. These results show that the speed oscillates over time and space but the oscillations are greater with HVs and AVs. The oscillations are smaller with automated vehicles, particularly CAVs. Further, the highest speed with HVs is 9.4 m/s, AVs is 10.7 m/s, and CAVs is 7.6 m/s. Thus, CAVs provide the best performance.

Figs. 6 and 7 give the proposed model acceleration and flow, respectively, with HVs, AVs, and CAVs for 150 s. These results show that the oscillations in acceleration and flow with HVs are large. For example, the acceleration varies between 0.73 m/s^2 and -1.67 m/s^2 from 0 s to 150 s. The acceleration oscillations with AVs are much smaller, i.e. between 0.53 m/s^2 and -1.00 m/s^2 from 53.5 s to 150 s. The corresponding flow varies between 0.002 and 0.009 from 56.0 s to 150 s and this is similar to the results for HVs. With CAVs the oscillations in acceleration are very small and the acceleration is approximately 0.002 m/s^2 from 16.0 s to 81.0 s.

Figs. 8, 9, and 10 present the traffic density behavior on a 1300 m road for 150 s with HVs, AVs, and CAVs, respectively. Fig. 8 shows that with HVs the density is large and oscillates over time and space between 0.20 and 0.04. Further, congestion occurs at regular intervals from 0 s to 150 s at several locations. With AVs, the oscillations in density are smaller, but congestion occurs as shown in Fig. 9. The density varies between 0.20 and 0.05 over time and space. The congestion with CAVs occurs from 0 s to 93.0 s at -117 m and decreases over time as shown in Fig. 10. After congestion dissipates, there are small changes in density between 0.03 and 0.09.

The results presented in this section show that AVs tend to maintain higher speeds on horizontal curves compared to HVs and CAVs. This is because AVs follow predefined rules and algorithms without human intervention and thus can navigate curves at higher speeds. However, at higher speeds horizontal curves can lead to traffic accidents as they are designed to facilitate gradual turns rather than fast maneuvers. Vehicles with higher speeds can misjudge the curvature, increasing the risk of accidents. HVs have lower speeds compared to AVs as drivers choose to reduce their speed due to safety concerns or uncertainty about the road ahead. However, HV speed oscillations are larger due to driver reaction to road conditions. CAVs have slower and more stable speeds compared to AVs and HVs as they prioritize safety and efficiency over speed. This results in smaller oscillations due to their ability to communicate with other vehicles and infrastructure.

Figs. 6 and 7 show that the variations in acceleration and flow with CAVs are much smaller than with HVs and AVs. In addition, CAVs have small densities as shown in Fig. 10 whereas HVs and AVs have large densities which result in congestion. Overall, the results obtained show that CAVs have better performance on horizontal curves compared to HVs and AVs.

3.2. Comparison of the proposed and ID models

In this section, the traffic behavior of the proposed and ID models is compared considering CAVs. CAVs are chosen as they have superior performance on horizontal curves. The simulation parameters in Table 1 are employed and a platoon of 25 vehicles is considered. Fig. 11 gives the spatial and temporal evolution of speed with CAVs for $\tau = 0.5, 1, 2$, and 2.5 s while Fig. 12 presents the corresponding time-space vehicle trajectories. When $\tau = 0.5$ s, the speed is zero, which results in congestion as the vehicles are not moving. At $\tau = 1$ s, congestion occurs from 0 s to 85.0 s. The vehicles move slowly and the maximum speed is 7.4 m/s. With $\tau = 2$ s, the congestion dissipates after 65.0 s and the vehicles move at speeds from 6.6 m/s to 17.2 m/s. At $\tau = 2.5$ s, the vehicles accelerate rapidly and reach a maximum speed of 21.2 m/s. There is no congestion after 70.5 s. Figs. 11 and 12 indicate that an increase in τ results in an increase in speed so vehicle dynamics are faster.

Fig. 13 gives the spatial and temporal evolution of speed with the ID model for $\delta = 1, 4$, and 80, and the corresponding time-space vehicle trajectories are presented Fig. 14. When $\delta = 1$, congestion occurs from 0 s to 57.5 s. Subsequently, vehicles move slowly and the maximum speed is 23.5 m/s. At $\delta = 4$, the congestion dissipates after 58 s and the vehicles move at speeds from 11.8 m/s to 27.5 m/s. At $\delta = 80$, congestion occurs from 0 s to 58 s, however, congestion occurs again after 140 s and increases over time. Figs. 13 and 14 indicate that an increase in δ results in an increase in speed and the appearance of congestion, which is not representative of real traffic dynamics.

4. Conclusion

Most traditional traffic models are based on fluid dynamics, but vehicle acceleration and deceleration behave like a spring-mass system. In this work, a microscopic traffic model was developed based on

Hooke's law for a spring-mass system to improve the ID model by addressing its limitations such as the unrealistic constant exponent δ and the dependence on fluid dynamics. This new model was used to investigate the behavior of HVs, AVs, and CAVs on horizontal curves as they are crucial for traffic safety and operational efficiency. The results obtained indicate that CAVs perform better than HVs and AVs on horizontal curves. In particular, the speed with CAVs is lower and more stable which allows for safer maneuvering. CAVs also have smaller speed and flow oscillations which reduces the probability of congestion. This is because CAVs can coordinate with other vehicles and infrastructure to adjust speeds and maintain a safe distance headway, resulting in a smooth flow. CAVs also have smaller acceleration and deceleration on horizontal curves which reduces fuel consumption and consequently traffic emissions, contributing towards a more sustainable transportation system. The comparison between the proposed and ID models indiates that the new model outperforms the ID model and provides more accurate and realistic traffic behavior. This work considered traffic behavior on horizontal curves during normal weather conditions. Future studies can expand the range of scenarios analyzed, including various road geometries and environmental conditions.

CRediT authorship contribution statement

Thomas Aaron Gulliver: Writing – review & editing, Validation, Funding acquisition, Visualization, Investigation, Formal analysis. **Faryal Ali:** Writing – original draft, Validation, Methodology, Formal analysis, Visualization, Software, Investigation, Conceptualization. **Ahmed B. Altamimi:** Visualization, Investigation, Writing – review & editing, Validation, Formal analysis. **Zawar Hussain Khan:** Writing – review & editing, Validation, Investigation, Formal analysis, Visualization, Methodology, Funding acquisition, Conceptualization.

Declaration of Competing Interest

The authors declare that they have no known competing financial interests or personal relationships that could have appeared to influence the work reported in this paper.

References

[1] Z. Cao, L. Lu, C. Chen, X.U. Chen, Modeling and simulating urban traffic flow mixed with regular and connected vehicles, IEEE Access 9 (2021) 10392–10399.

[2] J. Khoury, K. Amine, R.Abi Saad, An initial investigation of the effects of a fully automated vehicle fleet on geometric design, J. Adv. Transp. 2019 (2019) 6126408.

[3] M.M. Rana, K. Hossain, Connected and autonomous vehicles and infrastructures: A literature review, Int. J. Pavement Res. Technol. 16 (2) (2023) 264–284.

[4] S. Lam, J. Taghia, J. Katupitiya, Evaluation of a transportation system employing autonomous vehicles, J. Adv. Transp. 50 (8) (2016) 2266–2287.

[5] T. Vranken, B. Sliwa, C. Wietfeld, M. Schreckenberg, Adapting a cellular automata model to describe heterogeneous traffic with human-driven, automated, and communicating automated vehicles, Phys. A Stat. Mech. Appl. 570 (2021) 125792.

[6] M. Rahman, M.R. Islam, M. Chowdhury, and T. Khan, "Development of a connected and automated vehicle longitudinal control model," *arXiv*, 2019.

[7] D. Milakis, Long-term implications of automated vehicles: An introduction, Transp. Rev. 39 (1) (2019) 1–8.

[8] A. Talebpour, H.S. Mahmassani, Influence of connected and autonomous vehicles on traffic flow stability and throughput, Transp. Res. Part C. Emerg. Technol. 71 (2016) 143–163.

[9] Q. Wang, B. Li, Z. Li, and L. Li, "Effect of connected automated driving on traffic capacity," in *Proc. Chinese Automation Congress*, Jinan, China, 2017, pp. 633–637.

[10] D. Chen, S. Ahn, M. Chitturi, D.A. Noyce, Towards vehicle automation: Roadway capacity formulation for traffic mixed with regular and automated vehicles, in: Transp. Res. part B Methodol, 100, 2017, pp. 196–221.

[11] S.S. Washburn and L.D. Washburn, "Future Highways–Automated Vehicles," SunCam online continuing education course, Wellington, FL, USA, 2022. ⟨https://s3.amazonaws.com/suncam/docs/208.pdf⟩ (accessed Mar. 14, 2024).

[12] S. Pham, L. Truong, and N. Nguyen, "Impacts of autonomous vehicles on road and pavement design," in *Proc. Australasian Transport Research Forum*, Brisbane, QLD, Australia, 2021.

[13] Testbook, "Different Types of Curves in Surveying." ⟨https://testbook.com/civil-engineering/different-types-of-curves-in-surveying⟩ (accessed Mar. 14, 2024).

[14] Z. Binshuang, C. Jiaying, Z. Runmin, H. Xiaoming, Skid resistance demands of asphalt pavement during the braking process of autonomous vehicles, MATEC Web Conf. 275 (art. 04002) (2009).

[15] A. Abdulhafedh, Design of superelevation of highway curves: An overview and distribution methods, J. City Dev. 1 (1) (Sep. 2019) 35–40.

[16] S. Wang and B. Yu, "Impacts on the geometric design of highway from non-autonomous to autonomous vehicles," in *Proc. Transportation Research Board Annual Meeting*, Washington DC, USA, 2019.

[17] A.E. Adebisi, "A review of the difference among macroscopic, microscopic and mesoscopic traffic models," Technical Report, Department of Civil and Environmental Engineering, Florida A&M University, Tallahassee, FL, USA, 2016.

[18] C.M. Henein, T. White, Microscopic information processing and communication in crowd dynamics, Phys. A Stat. Mech. Appl. 389 (21) (Nov. 2010) 4636–4653.

[19] F. Ali, Z.H. Khan-, P. Eng, A. Altamimi, K. Khattak, T.A. Gulliver, A microscopic traffic model considering time headway and distance headway, Appl. Sci. 13 (12) (Jun. 2023) 7234 (art).

[20] Z.H. Khan, T.A. Gulliver, A macroscopic traffic model for traffic flow harmonization, Eur. Transp. Res. Rev. 10 (2) (Jun. 2018) 30.

[21] L.A. Pipes, An operational analysis of traffic dynamics, J. Appl. Phys. 24 (3) (1953) 274–281.

[22] A. Reuschel, Vehicle movements in a platoon, Oeste Ing. Arch. 4 (1950) 193–215.

[23] E. Kometani, T. Sasaki, On the stability of traffic flow (report-I), J. Oper. Res. Soc. Jpn. 2 (1) (1958) 11–26.

[24] L. Zhang, S. Zhang, B. Zhou, S. Jiao, Y. Huang, An improved car-following model considering desired safety distance and heterogeneity of driver's sensitivity, J. Adv. Transp. 2021 (Jan. 2021) 6693433.

[25] G.F. Newell, Nonlinear effects in the dynamics of car following, Oper. Res. 9 (2) (Apr. 1961) 209–229.

[26] F. Ali, Z.H. Khan-, P. Eng, K. Khattak, T.A. Gulliver, Evaluating the effect of road surface potholes using a microscopic traffic model, Appl. Sci. 13 (15) (Jul. 2023) 8677.

[27] M. Bando, K. Hasebe, A. Nakayama, A. Shibata, Y. Sugiyama, Dynamical model of traffic congestion and numerical simulation, Phys. Rev. E Stat. Phys. Plasmas Fluids Relat. Interdiscip. Top. 51 (2) (1995) 1035–1042.

[28] D. Helbing, B. Tilch, Generalized force model of traffic dynamics, Phys. Rev. E Stat. Phys. Plasmas Fluids Relat. Interdiscip. Top. 58 (1) (1998) 133–138.

[29] R. Wiedemann, "Simulation des Straßenverkehrsflusses," PhD dissertation, Univ., Inst. für Verkehrswesen, Karlsruhe, Germany, 1974.

[30] F. Ali, Z.H. Khan, K.S. Khattak, T.A. Gulliver, A.B. Altamimi, A microscopic traffic model incorporating vehicle vibrations due to pavement condition, Mathematics 11 (24) (2023) 4911.

[31] S. Krauß, P. Wagner, C. Gawron, Metastable states in a microscopic model of traffic flow, Phys. Rev. E Stat. Phys. Plasmas Fluids Relat. Interdiscip. Top. 55 (5) (1997) 5597.

[32] D. Salles S. Kaufmann H. Reuss Extending the intelligent driver model in SUMO and verifying the drive off trajectories with aerial measurements *Proc. SUMO Users Conf.* Oct. 2020.

[33] M. Treiber, A. Hennecke, D. Helbing, Congested traffic states in empirical observations and microscopic simulations, Phys. Rev. E Stat. Phys. Plasmas Fluids Relat. Interdiscip. Top. 62 (2) (2000) 1805–1824.

[34] F. Zong, M. Wang, M. Tang, X. Li, M. Zeng, An improved intelligent driver model considering the information of multiple front and rear vehicles, IEEE Access 9 (2021) 66241–66252.

[35] A. Jafaripournimchahi, Y. Cai, H. Wang, L. Sun, J. Weng, Integrated-hybrid framework for connected and autonomous vehicles microscopic traffic flow modelling, J. Adv. Transp. 2022 (2022) 2253697.

[36] Q. Xin, R. Fu, W. Yuan, Q. Liu, S. Yu, Predictive intelligent driver model for eco-driving using upcoming traffic signal information, Phys. A Stat. Mech. Appl. 508 (2018) 806–823.

[37] M.J. Lighthill, G.B. Whitham, On kinematic waves II. A theory of traffic flow on long crowded roads, Proc. R. Soc. Lond. Ser. A. Math. Phys. Sci. 229 (1178) (1955) 317–345.

[38] P.I. Richards, Shock waves on the highway, Oper. Res. 4 (1) (1956) 42–51.

[39] Z.H. Khan, T.A. Gulliver, A macroscopic traffic model based on anticipation, Arab. J. Sci. Eng. 44 (5) (2019) 5151–5163.

[40] H.J. Payne, "Models of freeway traffic and control," in *Proc. Mathematical Models of Public Systems*, Raleigh, NC, USA, pp. 51–61, 1971.

[41] G.B. Whitham, Linear and Nonlinear Waves, Wiley, New York, NY, 1971.

[42] C.F. Daganzo, Requiem for second-order fluid approximations of traffic flow, Transp. Res. Part B 29 (4) (1995) 277–286.

[43] T. Nagatani, Modified KdV equation for jamming transition in the continuum models of traffic, Phys. A Stat. Mech. Appl. 261 (3–4) (1998) 599–607.

[44] T. Nagatani, Jamming transition of high-dimensional traffic dynamics, Phys. A Stat. Mech. Appl. 272 (3–4) (1999) 592–611.

[45] A. Abbas, A. Khan, T. Abdeljawad, M. Aslam, Numerical simulation of variable density and magnetohydrodynamics effects on heat generating and dissipating Williamson Sakiadis flow in a porous space: Impact of solar radiation and Joule heating, Heliyon 9 (11) (2023).

[46] A. Abbas, et al., Effect of non-uniform heat rise/fall and porosity on MHD Williamson hybrid nanofluid flow over incessantly moving thin needle, Heliyon 10 (1) (2024).

[47] Y. Li, W. Chen, S. Peeta, X. He, T. Zheng, H. Feng, An extended microscopic traffic flow model based on the spring-mass system theory, Mod. Phys. Lett. B 31 (09) (2017) 1750090.

[48] F. Kessels, Traffic Flow Modelling: Introduction to Traffic Flow Theory Through a Genealogy of Models, Springer, Cham, Switzerland, 2018.

[49] H. Halim, S.A. Adisasmita, M.I. Ramli, S.H. Aly, The relationship of volume and headway on heterogen traffic conditions in Makassar City, IOP Conference Series Earth Environmental Science 419 (012105) (2020).

[50] G. Elert, "Equations of Motion," in The Physics Hypertextbook. ⟨https://physics.info/motion-equations/⟩ (accessed Mar. 14, 2024).

[51] ESE Notes, "Transition Curves & Length of Transition Curve 2.20." ⟨https://esenotes.com/transition-curves-length-of-transition-curve/⟩ (accessed Feb. 21, 2024).

[52] BigRentz, "What Is Superelevation and How Does It Keep Roads Safer?" ⟨https://www.bigrentz.com/blog/superelevation⟩ (accessed Feb. 13, 2024).

[53] G. Xu, et al., The influence of the pavement friction coefficient evolution caused by traffic flow on the risk of motorway horizontal curves, PLoS One 17 (8) (2022).

[54] Federal Highway Administration, "Mitigation Strategies For Design Exceptions - Superelevation." ⟨https://safety.fhwa.dot.gov/geometric/pubs/mitigationstrategies/chapter3/3_superelevation.cfm⟩ (accessed Feb. 13, 2024).

[55] A.A. Kordani, O. Rahmani, A.S.A. Nasiri, S.M. Boroomandrad, Effect of adverse weather conditions on vehicle braking distance of highways, Civ. Eng. J. 4 (1) (Feb. 2018) 46–57.

[56] Physics 101 The Physics of How Things Work: Tire Friction." ⟨http://boson.physics.sc.edu/~rjones/phys101/tirefriction.html⟩ (accessed Feb. 17, 2024).

[57] M. Taieb-Maimon, D. Shinar, Minimum and comfortable driving headways: Reality versus perception, Hum. Factors 43 (1) (2001) 159–172.

[58] Smart Motorist, "How Long Is A Car? (Average Car Length According to Types)." ⟨https://www.smartmotorist.com/average-car-length⟩ (accessed May 8, 2022).